www.cad-journal.net
Computer-Aided Design AND APPLICATIONS

Comparison of Multi-Objective Optimization Algorithms for Generative Design: Performance Evaluation in Custom Dental Abutment Design

Petar Kosec[1,2], Jonny Binder[3], Tomislav Martinec[4] and Stanko Škec[5]

[1] University of Zagreb, Croatia, Faculty of Mechanical Engineering and Naval Architecture, petar.kosec@fsb.hr
[2] Neo Dens Ltd., Zagreb, Croatia, petar.kosec@neo-dens.hr
[3]University of Leeds; Paxman Scalp Cooling, pszx1778@leeds.ac.uk
[4]University of Zagreb, Croatia, Faculty of Mechanical Engineering and Naval Architecture, tomislav.martinec@fsb.hr
[5]University of Zagreb, Croatia, Faculty of Mechanical Engineering and Naval Architecture, stanko.skec@fsb.hr

Corresponding author: Petar Kosec, petar.kosec@fsb.hr

Abstract. This study explores how different multi-objective optimization algorithms interact with a parametric model in the context of explicit generative design. A parametric model of a custom dental abutment was optimized using NSGA-III, MOEA/D, and RBFMOpt, representing Pareto-based, decomposition-based, and surrogate-assisted strategies. Applied to two clinical cases, the algorithms targeted five geometric objectives derived from anatomical and prosthetic requirements. Results show that local objectives converged quickly, while global objectives were more complex due to non-linear parameter interactions. NSGA-III offered the most consistent performance, while RBFMOpt showed early precision and MOEA/D struggled with objective coupling. The findings highlight the importance of parametric model preparation, emphasizing localized control, hierarchy, and parameter bounding. Future work will explore hybrid and data-driven generative strategies, expanded objective sets, and alternative model configurations to guide more robust design workflows.

Keywords: generative design; parametric design; multi-objective optimization; dental abutment
DOI: https://doi.org/10.14733/cadaps.2026.532-551

1 INTRODUCTION

Generative design (GD) refers to a class of computational methods that algorithmically generate and evaluate multiple design alternatives based on a set of predefined goals and constraints [6]. These methods are particularly effective when the design space is high-dimensional, interdependent, or otherwise impractical to explore manually [25]. By automating the generation of design variants and assessing them against performance objectives, GD expands the solution space available to the designer and supports more informed decision-making [33].

GD methods are typically categorized as data-driven (AI-driven) and explicit (parametric) based on how the design space is defined and explored. Data-driven GD employs machine learning models, such as generative adversarial networks (GANs) or variational autoencoders (VAEs), trained on large datasets of existing designs [44]. These models can generate novel geometries by learning patterns from the training data, enabling rapid exploration of alternative design directions. While this approach supports diversity and early-stage ideation, it offers limited precision and control over geometry and is less compatible with rule-based engineering workflows [1]. In contrast, in explicit GD, the designer creates a parametric model in which geometry, model constraints, and performance objectives are explicitly defined. The structured design space is explored by optimization algorithms that systematically vary selected input parameters. Each generated variant is then evaluated against the predefined objectives, such as minimizing weight, maximizing stiffness, or achieving specific dimensional

targets, using performance metrics derived from simulation, geometric analysis, or rule-based criteria. This approach offers high geometric control, compatibility with CAD environments, and facilitates integration of functional and manufacturing requirements, making it well-suited for constrained mechanical design tasks.

As GD becomes more integrated into engineering and product development workflows [2,40,44], attention is shifting from algorithm performance to the preparatory phase, particularly in explicit methods, where model setup strongly influences generative outcomes [4,38]. While much of the existing literature focuses on solver behavior and GD tools capabilities [19,49], the effectiveness of GD often depends on how the model is structured: how parameters are defined, how interdependencies are handled, and how constraints and objectives are embedded into the geometry which is rarely explained in existing studies.

In this study, three different GD algorithms—NSGA-III, MOEA/D, and RBFMOpt—are applied to a parametric model developed for two industrial cases involving custom dental abutments. Algorithmic behavior was compared in terms of convergence dynamics, solution variety, and the interaction between parameter structure and optimization strategy. These comparisons provided insights into aspects of model preparation, including parameter hierarchy, model segmentation, constraint definition, and sensitivity management. While case studies involve a custom dental abutment, the focus is not on dental-specific optimization. Instead, this parametric model is treated as a representative example of a constrained, personalized mechanical component. The insights gained from this study are intended to support design engineers working in similarly complex, performance-driven design contexts where parametric modeling and generative algorithms must be combined effectively. The paper is organized as follows: Section 2 presents background concepts and related work. Section 3 details the methodology, including the parametric model structure, optimization setup, and evaluation framework. Section 4 presents the results of the generative optimization runs. Section 5 discusses the observed algorithmic behaviors in relation to model structure. Finally, Section 6 concludes the paper and outlines directions for future work.

2 BACKGROUND AND RELATED WORK

GD emerged as a design method intended to assist designers in systematically surveying and exploring the design space [32]. Rather than iterating manually, the designer defines a design space and allows the algorithm to explore it, autonomously proposing variations that are then evaluated against performance metrics. This results in a wider, faster, and potentially more innovative exploration of solutions than would be feasible using conventional design workflows. In the context of engineering, GD addresses several persistent challenges: increasing product complexity, tighter performance and regulatory requirements, shortened development cycles, and the growing demand for highly customized yet functional products [28,38]. Traditional CAD-based approaches depend heavily on designer intuition, expert knowledge and manual iteration, which can become limiting when solutions span high-dimensional or interdependent parameter spaces. GD shifts the designer's role toward setting up design logic and evaluation rules while allowing the algorithm to handle large-scale variation and selection [45].

GD typically integrates three interdependent components: a design representation, a definition of objectives and constraints, and an optimization strategy [9]. In the context of GD, the design representation defines how the solution space is formulated and navigated—ranging from parametric models to voxel grids, density fields, shape grammars, graph-based structures, etc. [44,53]. This choice determines not only the flexibility of the model but also how constraints and evaluations can be applied. Objectives and constraints provide the evaluative logic that guides the generative process, ensuring that design alternatives are not only diverse but also functional and manufacturable [31]. These can include performance-related metrics such as strength-to-weight ratio, energy efficiency, or cost, as well as geometric, regulatory, or process-based constraints that enforce feasibility. The third critical element is the optimization strategy, which determines how the design space is explored and refined [19]. The effectiveness of the generative process depends heavily on the match between the optimization strategy and the characteristics of the design problem [12]. While these three components are conceptually distinct, their integration is essential for enabling robust generative workflows that are both creative and technically rigorous.

In practical workflows, GD serves both as an ideation tool and as an optimization framework. In early design stages, it supports creative exploration by rapidly producing geometric alternatives [45]. In later stages, it becomes a formal method for refining design candidates to meet different targets such as geometry, manufacturability, weight, structural, cost, and similar [24,48]. The rise of integrated design environments (e.g., Rhino3D/Grasshopper, Autodesk Fusion, nTopology, Solidedge, Solidworks) has further enabled the adoption of GD by embedding parametric modeling, simulation, and optimization tasks within a single ecosystem [20,41,43]. These platforms reduce barriers to entry and enable designers to build, explore, and iterate on generative workflows with increasing speed and precision. However, algorithms operate within the logical framework defined by the designer [39]. GD should therefore not be viewed as a form of full design automation, but rather as an exploratory and evaluative aid capable of revealing non-intuitive solutions, yet fundamentally dependent on the modeling decisions and intent encoded by the engineer.

The effectiveness of GD is highly influenced by the way the parametric model is defined, specifically, how parameters are selected, how the model structure supports variation, and how design constraints are implemented. Recent studies have emphasized that the organization, robustness, and clarity of the parametric model plays a pivotal role in determining the quality and convergence of generative outputs. Harding and Shepherd [23] demonstrated that the definition order of parameters, the modularization of geometry, and the hierarchy of dependencies directly affect the reliability of generative iterations. Mountstephens and Teo [37] concluded that weak constraint propagation and poorly defined parameter logic are leading causes of model failure during algorithmic runs. Li et al. [33] showed through comparative analysis that poorly structured parametric models lead to reduced solution diversity and lower fidelity outcomes in constrained design spaces. Gu et al. [21] argued that the geometric and parametric positioning of the initial genotype, particularly its location relative to the center of the design space, has a measurable effect on the algorithm's ability to efficiently traverse the solution space. Starodubcev et al. [47] reported that inadequate coupling between parameters and evaluation criteria is a major barrier to convergence and increases the likelihood of infeasible or geometrically invalid outputs. Belluomo et al. [3] similarly concluded that many GD failures originate not in the algorithm itself but in ill-prepared parametric models lacking constraint-aware segmentation and scalable feature logic. Cirello et al. [13] showed that in orthopedic product development, generative workflows required precise model segmentation and robust geometric constraints to function effectively. Likewise, Chen et al. [11] highlighted that embedding functional relationships directly into parametric logic enhances both geometric integrity and the algorithm's ability to respond to performance-based objectives. Together, these findings reinforce that generative algorithms do not operate in isolation; their performance is fundamentally shaped by the structure, clarity, and constraint logic of the model they interact with.

A robust parametric model does not guarantee successful outcomes. The quality and behavior of the generative results also depend significantly on the chosen optimization algorithm [42,46]. A critical factor in algorithm choice is whether the design task involves a single or multiple, potentially conflicting objectives. In single-objective optimization, the algorithm targets a specific performance metric, such as stiffness, weight, or cost, using strategies like gradient-based methods or evolutionary searching [15]. In contrast, multi-objective optimization (MOO) aims to find a set of solutions that balance competing criteria, approximating the Pareto front [26]. Multi-objective algorithms are especially valuable in engineering contexts, where a single solution often does not satisfy all objectives and trade-offs between objectives are unavoidable [2].

Despite the importance of aligning algorithm choice with parametric model structure, algorithm selection is often treated as a secondary decision. Many GD studies emphasize final output, evaluating convergence metrics, design variety, or how distinct or unconventional the generated forms appear, without analyzing the mechanisms by which those results were achieved [38]. Specifically, the internal dynamics of optimization, how algorithms traverse parameter space, interpret constraint boundaries, or evolve solutions, are rarely examined in relation to the underlying model. Most comparative studies are conducted on mathematically idealized benchmark problems, which offer clear analytical properties but do not capture the constraint complexity, geometry sensitivity, or interdependent variables typical in real engineering contexts. As such, algorithmic behavior observed in benchmarks may not generalize to realistic use cases involving CAD-based parametric models. In industrially relevant cases, especially in mechanical or biomedical design, the search space is rarely smooth, convex, or uniformly defined [7]. It often involves nonlinear constraints, piecewise geometric transitions, or objective formulations that depend on specific functional requirements [13,51]. Under such conditions, minor changes in parameter values can result in geometric failure, constraint violation, or convergence breakdowns. Moreover, different algorithms interact with the same model in fundamentally different ways, some prioritizing local refinement, others global exploration, depending on how they encode variation, assess feasibility, and manage trade-offs [8]. The lack of literature examining this interaction leaves a critical gap in understanding. Without empirical analysis of how optimization algorithms engage with structured parametric models in real-world workflows, designers are left with limited guidance on how to tune, adapt, or select algorithms for specific use cases. As a result, there is no systematic framework for understanding how solution quality arises, not only from the capabilities of the algorithm or the structure of the model individually, but from their alignment. Performance depends not just on how well each component is designed, but on how effectively the algorithm can navigate and exploit the model's structure.

To understand how optimization algorithms influence GD outcomes, it is necessary to examine the strategic mechanisms these algorithms use to explore the solution space and evaluate candidate designs. In generative workflows, particularly those involving explicit parametric models, the search process is not simply about identifying optimal solutions, but about navigating a space defined by a parametric model. Each family of optimization algorithms brings different assumptions and search strategies, which affect how thoroughly the design space is explored and how well trade-offs are managed. Three prominent families of optimization strategies have emerged in the context of GD: Pareto-based algorithms, decomposition-based algorithms, and surrogate-assisted algorithms [49]. These represent fundamentally different approaches to managing multi-objective search and are widely used in both academic studies and commercial design tools.

Pareto-based algorithms operate by evolving a population of candidate solutions and evaluating them based on non-dominance principles, treating each objective as equally important and allowing trade-offs to emerge naturally through population competition [16]. This approach is capable of discovering non-convex and discontinuous Pareto fronts, making it suitable for problems where objectives are in tension and no clear weighting exists [27]. Among Pareto-based algorithms, NSGA-III (Non-dominated Sorting Genetic Algorithm III) is particularly notable for introducing reference-point-based selection to promote uniform distribution along the Pareto front [17]. It partitions the objective space using predefined directions, maintaining diversity even when optimizing three or more conflicting objectives. In the context of explicit GD, NSGA-III's ability to explore and maintain a wide range of trade-offs without scalarization makes it highly effective when complex, interdependent objectives are present.

Decomposition-based algorithms reformulate the multi-objective problem into a set of scalar subproblems, each corresponding to a specific trade-off direction [52]. Solutions are evolved locally around these subproblems, and neighborhood-based information sharing is used to improve convergence and maintain diversity. MOEA/D (Multi-Objective Evolutionary Algorithm based on Decomposition) exemplifies this strategy, where each individual optimizes a subproblem associated with a particular weight vector [18]. The method is effective in scenarios where directional control of solution exploration is desirable and where trade-offs between objectives are approximately known. In constrained GD, MOEA/D offers a more structured and localized search behavior, which can be advantageous when parametric changes produce localized effects on geometric outcomes [34]. However, decomposition methods may struggle when objectives are highly nonlinear or when dominant relationships between objectives are complex and discontinuous.

Surrogate-assisted algorithms approach the challenge of optimization efficiency in cases where each true evaluation is resource-expensive. Rather than evaluating every candidate solution through full computation, they construct surrogate models that approximate the objective functions based on previously evaluated points [22]. New candidate solutions are proposed by querying the surrogate, and only promising solutions are evaluated with the true objective function [50]. RBFMOpt, used in this study, applies radial basis function interpolation to construct such a surrogate landscape [14]. It proposes solutions based on predicted performance, selectively validates them against the real mathematical model, and iteratively refines the surrogate. This approach greatly reduces evaluation costs, making it particularly suitable for GD workflows where geometry regeneration, constraint checking, and objective measurements are time intensive [35]. The effectiveness of surrogate-assisted optimization depends heavily on the accuracy of the surrogate model, which is influenced by the underlying model structure, the overall complexity of the design space, and the representativeness of the initial surrogate [5].

To represent the three major optimization strategies, NSGA-III, MOEA/D, and RBFMOpt were selected and implemented within the same parametric model and generative environment, using consistent parameter settings to ensure a controlled basis for comparison. Each algorithm introduces a distinct approach to optimization and search dynamics, influencing how design space exploration unfolds during the generative process. The objective of this study is not only to evaluate differences in performance metrics or Pareto front quality, but also to observe how each algorithm interacts with the structure of the parametric model: how constraints are handled, how variations are managed, and how the algorithm's internal search logic aligns, or conflicts, with the organization of the design space. By analyzing these interactions, the study aims to generate deeper insights into the relationship between algorithmic behavior and parametric model design, and to understand how this relationship shapes GD outcomes in constrained multi-objective engineering tasks.

3 METHODOLOGY

This section outlines the approach used to evaluate how different GD algorithms perform when applied to a unified, explicitly constrained parametric model. The product selected for this study is a custom dental abutment, representing individualized mechanical components that must conform to both anatomical and technical requirements. GD in this study is primarily focused on geometrical performance objectives, such as fit, alignment, and surface adaptation, while manufacturability constraints, though not explicitly optimized, are partially addressed through embedded geometric limitations. Rather than isolating algorithmic capabilities or relying on simplified models, the methodology is grounded in a realistic design scenario that imposes spatial constraints and structural interdependencies. The study is structured to reveal how differences in algorithmic search strategy manifest when operating on the same parametric model. To that end, the following subsections describe the selected case study, the structure and segmentation of the parametric model, and the experimental setup for evaluating each algorithm under controlled yet practically relevant conditions.

3.1 Case Study Overview

A dental abutment functions as a connector between a dental implant, a fixture surgically inserted into the jawbone, and the prosthetic restoration, such as a crown, bridge, or denture (Figure 1, left). It is a non-visible, subgingival component that must provide a secure mechanical interface between the implant and prosthetic,

while supporting the surrounding soft tissue and ensuring proper alignment, stability, and aesthetic emergence of the final tooth restoration.

The geometric design of a dental abutment is defined by clinical, tooth-specific morphological, and patient-specific requirements. The abutment must integrate precisely with the implant system using predefined interface geometries and must adapt to the unique anatomical and spatial conditions present in the patient's oral cavity. For these reasons, dental abutments are customized components, designed on a per-case basis by dental technicians using CAD systems. Their geometry is driven by restorative planning, soft tissue depth, implant angulation, occlusal space, and prosthetic alignment.

Functionally, a dental abutment can be divided into three distinct segments (Figure 1, right):

- The Implant Connection Segment (ICS) is the region that connects with the internal geometry of the implant. This segment must remain non-customizable and must comply with implant manufacturer specifications. It ensures the mechanical locking and sealing functions of the abutment–implant connection.
- The Transgingival Segment (TGS) defines the emergence margin curve of the restoration through the soft tissue. Its geometry is subgingival, and it must adapt to the contour of the gingiva, supporting soft tissue in a biologically favorable way while maintaining adequate wall thickness (for titanium alloy - min 0,4mm) and smooth geometric transitions.
- The Prosthetic Connection Segment (PCS) supports the visible prosthetic component and includes the screw channel or cementation surface. This segment must align with the prosthetic crown, follow interproximal and occlusal spatial constraints, and provide sufficient bonding or retention area.

Because the ICS must remain fixed and unaltered, only the TGS and PCS are candidates for parametric modeling and generative variation. These regions introduce complexity in both geometry and constraints, making the abutment a suitable case for evaluating GD workflows that require explicit parametric control and multi-objective optimization.

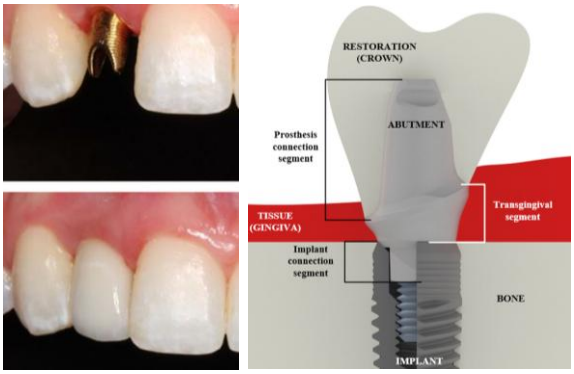

Figure 1. Dental abutment mounted on an implant in patient's jaw– left [29]; Dental abutment segments [30].

To ensure consistency in model structure and to enable comparative evaluation of algorithmic behavior, a single parametric model was constructed and tested on two clinically distinct cases:

- CASE 1 - involving tooth position 15 (a posterior premolar),
- CASE 2 - involving tooth position 21 (an anterior incisor).

These two positions represent different spatial and functional design contexts. The posterior case (tooth 15) allows for wider and mechanically robust geometries, with relatively uniform gingival profiles. In contrast, the anterior case (tooth 21) introduces constraints related to aesthetics, requiring the abutment to be submerged deeper under the gingival tissue, as well as limited interproximal space.

This case study serves a dual role: it represents a technically constrained real-world component, and it provides a structured context for analyzing how generative algorithms interact with an explicitly defined parametric design space. The following section describes how this parametric model was structured, including segmentation, parameter definition, constraint logic, and the model's integration with the optimization process.

3.2 Parametric Model Structure

The parametric model used in this study was developed in Rhino3D using Grasshopper, a visual programming environment commonly used for GD [4]. The model was designed to explicitly represent the geometric variability of the TGS and PCS of a dental abutment, while keeping the ICS fixed and non-editable. The TGS and PCS were defined as parametric surfaces, generated from a minimal set of functional and geometry-driving parameters.

These two regions were modeled independently but maintained continuity through shared boundary conditions, ensuring a consistent transition in geometry during generative exploration. To manage constraint propagation and ensure model robustness, the model was structured hierarchically. Parameters defining the TGS were defined first and used to generate a control curve representing the emergence margin curve. The PCS was then constructed from the upper boundary of the TS, with parameters influencing its height, angulation, taper, and shoulder width. This ordered definition ensures that downstream geometry is built on valid upstream conditions, reducing the likelihood of failure during parameter changes. In this model, the TGS is defined based on four prosthetic surfaces corresponding to standard anatomical directions: distal, mesial, buccal, and oral [10] (Figure 2).

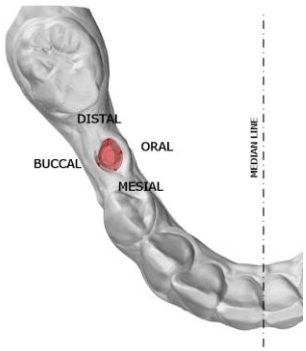

Figure 2. Prosthetics and tissue surfaces (right).

Four points are defined, one for each prosthetic surface. These four points together define a closed gingival margin curve. Each reference point is described by two geometric parameters:

- Lateral offset from the ICS origin along the X- and Y-axes: Y_d, Y_m, X_o, X_b
- Vertical height from the ICS interface along the Z-axis: Z_d, Z_m, Z_o, Z_b

These define the control geometry for the TGS (Figure 3), yielding eight parameters that describe the position and shape of the gingival margin curve. The four points are used to generate interpolated curve (via the *InterpCrv* component), defining the perimeter of the gingival margin in both planar and vertical orientations. These curves are then combined to create a closed loop, serving as the upper boundary of the TGS surface. The TGS is formed as a lofted surface from the implant platform (defined by a fixed base circle) to this upper boundary.

Two global parameters define the geometry at the connection between the TGS and ICS: the vertical position of the implant platform (Z = 0) and the diameter of the base circle (BD = 2,2 mm). These values are fixed and applied identically in both test cases to maintain consistency in implant interface conditions. Additional parameters refine the transition between the ICS and the anatomical emergence margin curve. The TGS_{IP} controls the vertical location of the inflection point along the TGS surface, enabling a smooth transition from the circular implant interface to the asymmetrical gingival margin. The TGS_{VTH} parameter defines the minimum vertical thickness at the emergence margin curve of the abutment to prevent thin-walled geometries that could pose mechanical or manufacturing problems.

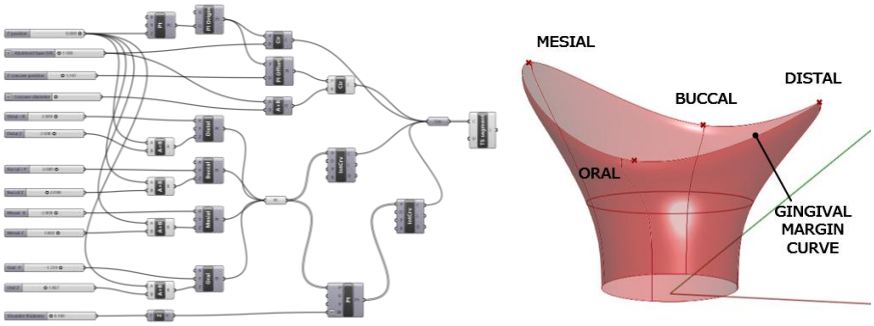

Figure 3. Canvas of TGS in Grasshopper and CAD model in Rhino3D

The PCS is designed based on a vector defined by three parameters:

- A_X (Angulation X) – controls the tilt of the PCS axis in the mesio-distal direction,
- A_Y (Angulation Y) – controls the tilt in the bucco-oral direction,

- *CH* (Prosthetic height) – defines the length of the segment from the gingival margin to the prosthetic platform.

The parameters A_X and A_Y are used to define the tilt of the vector that establishes the orientation of the PCS. This vector determines the direction in which the segment extends, allowing the PCS to vary its inclination while maintaining consistency in the base geometry inherited from the TGS. The PCS geometry is designed using a ruled surface between two curves. The first curve is an offset of the TGS emergence margin curve, which serves as the base of the PCS. The second curve is generated by projecting the emergence margin curve along the tilted vector to a plane intersecting the endpoint of the PCS, followed by an inward offset to maintain wall thickness and functional proportions. This approach enables smoother transitions and controlled tapering of the supragingival surface. Two additional parameters are defined: shoulder width (PCS_{SW}), which specifies the radial width at the transition between the TGS and PCS and is linked to the minimum required wall thickness for the prosthetic structure, and PCS draft (PCS_D) which influences the structural integrity and assembly characteristics of the prosthetic component mounted onto the abutment. The resulting parametric implementation of the PCS ensures geometric continuity with the TGS (Figure 4) and provides a flexible yet stable model for generative design exploration, supporting controlled variation of prosthetic angulation, height, and taper under predefined constraints.

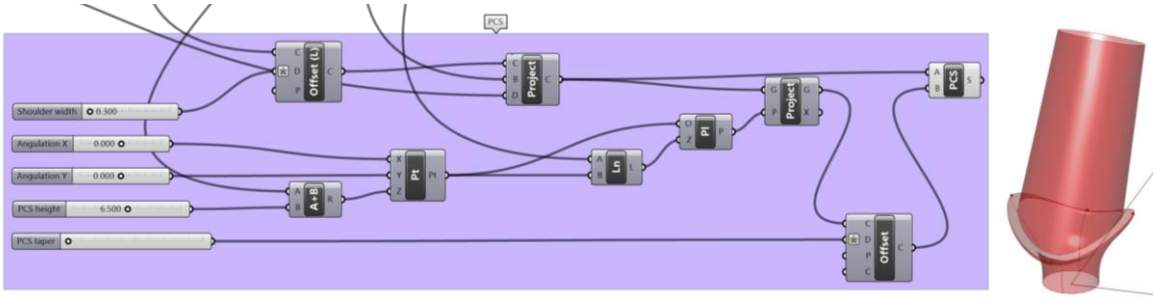

Figure 4. Canvas of PCS in Grasshopper and TGS CAD model in Rhino3D.

3.3 Integration of GD Algorithms with the Parametric Model

Before generative design algorithms can be applied to a parametric model, several preparatory steps must be completed to define a well-structured and bounded design space, one that allows meaningful exploration while remaining within feasible geometric and functional limits. These include [36] :

1. selecting which parameters are used as variables in the optimization process,
2. defining valid parameter ranges to constrain the search space and ensure geometric and functional feasibility,
3. establishing performance objectives, which guide the algorithm's evaluation of design alternatives and are aligned with the initial functional and design requirements of the product.

Rather than treating the model as a black box, the aim was to explicitly define which parameters were subjected to generative exploration and which were kept fixed, based on their geometric role, clinical relevance, and potential to affect the robustness of geometric constraints or functional validity of the model. For each parameter selected for optimization, ranges were defined to limit the search space to geometrically valid and clinically acceptable values. These ranges were derived from baseline designs produced by dental technicians in conventional dental CAD tools supplemented by anatomical constraints. The selected parameters and their defined intervals (Table 1 and Figure 5) were then used as input variables for the optimization algorithms.

Parameter	Description	Segment	Parameter range
X_o	Lateral offset of emergence margin curve from ICS diameter in X axis direction on the oral side of the abutment/jaw scan	TS	-1mm to -3mm
X_b	Lateral offset of emergence margin curve from ICS diameter in X axis direction on the buccal side of the abutment/jaw scan	TS	+1mm to +3mm
Y_d	Lateral offset of emergence margin curve from ICS diameter in Y axis direction on the distal side of the abutment/jaw scan	TS	-1mm to -3mm
Y_m	Lateral offset of emergence margin curve from ICS diameter in Y axis direction on the mesial side of the abutment/jaw scan	TS	+1mm to +3mm

Z_o	Vertical offset of emergence margin curve from ICS in Z direction on oral side of the abutment/jaw scan	TS	0 to +5mm
Z_b	Vertical offset of emergence margin curve from ICS in Z direction on buccal side of the abutment/jaw scan	TS	0mm to +5mm
Z_d	Vertical offset of emergence margin curve from ICS in Z direction on distal side of the abutment/jaw scan	TS	0mm to +5mm
Z_m	Vertical offset of emergence margin curve from ICS in Z direction on mesial side of the abutment/jaw scan	TS	0mm to +5mm
A_x	Horizontal offset of the PCS apex point in Y axis (angulation around X axis)	PCS	-2mm to +2mm
A_y	Horizontal offset of the PCS apex point in X axis (angulation around Y axis)	PCS	-2mm to +2mm
CH	PCS height	PCS	+3 to +10mm

Table 1. List of selected parameters for optimization and their parameter ranges.

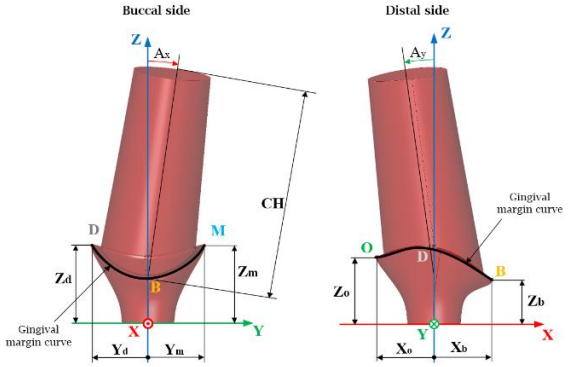

Figure 5. Abutment design parameters optimized by algorithms.

TGS parameters selected for implementing in GD algorithms allow adaptation to different tissue profiles while maintaining surface continuity. As these parameters define the emergence margin curve, one of the most anatomically sensitive and variable aspects of the abutment, they are well-suited for generative design. The PCS parameters collectively define the orientation and extent of the PCS. Their inclusion enables the algorithm to explore different prosthetic configurations and adapt the abutment to case-specific spatial and alignment constraints, such as the available vertical height between the implant and the opposing dentition, the distance to adjacent teeth, and the inclination of the natural tooth axis inferred from neighboring structures. By adjusting the height and angulation of the PCS, the GD algorithm can account for both functional clearance and anatomical integration requirements.

Four parameters were excluded from GD: TGS_{VTH}, TGS_{IP}, PCS_{SW}, and PCS_{D}. As the focus of this research is on optimizing geometric performance rather than manufacturing, structural, or assembly-related objectives, these parameters were reserved for manual adjustment and fine-tuning by the designer to ensure control over critical functional features.

The final step in preparing the parametric model for generative design was the definition of performance objectives, which guide the evaluation of each generated design. In this study, performance objectives were defined based on clinical and functional requirements and evaluated through geometric relationships between the abutment and the surrounding anatomical structures. This ensured that the generated solutions respected spatial constraints and fulfilled case-specific design goals. In the Grasshopper environment, the optimization objectives were implemented through a system of dynamic geometric measurements linking the parametric model to the patient's anatomical scan. To establish a reference framework, specific anatomical surfaces are manually identified on the digital scan of the patient's jaw. Four reference points were placed to correspond to the distal (D), buccal (B), mesial (M), and oral (O) directions relative to the implant site (Figure 6, left), representing key locations where the emergence margin curve of the abutment must integrate smoothly with the surrounding soft tissue. Within the parametric abutment model, the corresponding points were generated based on the geometry of the gingival margin curve for the TGS. As the parametric model regenerated for different parameter combinations, these model points moved accordingly, maintaining a direct link to the generative parameters under optimization. Using Grasshopper's *Distance* components, Euclidean distances were

dynamically calculated between each pair of model and scan reference points. These four distances resulted in four objectives (O1–O4) captured the deviation between the TGS emergence margin curve and the soft tissue surface, ensuring anatomical integration.

For the PCS-related objective (O5), two points were manually placed at the top regions of the adjacent teeth, one on the mesial surface of the neighboring tooth and one on the distal surface of the opposite neighboring tooth. A midpoint between these two adjacent reference points was defined and used as the spatial target for the PCS apex (Figure 6, right). The apex of the PCS, generated based on the angled extrusion defined by the Ax, Ay, and H parameters, was compared against this midpoint by calculating the Euclidean distance. This setup allowed the PCS to be evaluated not only for vertical height but also for alignment relative to the adjacent dental structures, which is clinically critical for ensuring proper prosthetic emergence, access for prosthetics insertion, and maintenance of contact points.

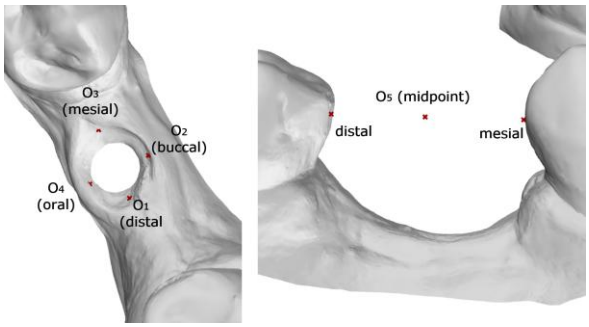

Figure 6. Reference points defining objectives for multi-objective optimization.

Objectives O1-O5 were evaluated continuously during the GD process, providing real-time feedback to the optimization algorithms (Figure 7). Minimizing these distances simultaneously posed a multi-objective optimization challenge, as improving the fit in one region could compromise alignment elsewhere. By structuring the evaluation through direct spatial relationships between the parametric model and the anatomical context, the optimization process remained grounded in clinically meaningful geometry, ensuring that the generated solutions were assessed not only by internal parametric logic but also by their anatomical integration within the patient-specific environment.

While it is theoretically possible to design abutment geometry by directly fitting to anatomical scan data to minimize distances (O1–O5), such an approach would neglect important design constraints and functional requirements. Generative optimization enables systematic trade-off exploration across competing objectives while ensuring geometric validity and compliance with clinical constraints embedded in the parametric model. Therefore, minimizing the five distance-based objectives through generative variation provides a clinically meaningful balance between anatomical adaptation and functional design performance.

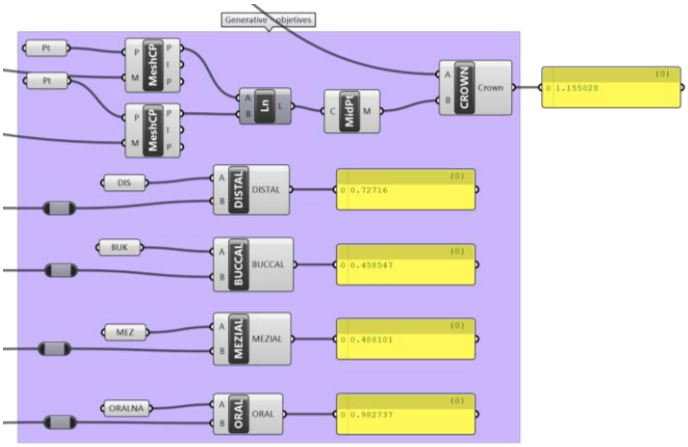

Figure 7. Setup of GD optimization objectives in Grasshopper.

Multi-objective optimization was performed using two separate optimization plugins:

- NSGA-III optimization was implemented using the Tunny plugin.
- MOEA/D and RBFMOpt were implemented using the Opossum plugin

Tunny was selected due to its direct support for multi-objective evolutionary algorithms based on the NSGA-III framework, enabling Pareto-based optimization with reference-point-guided diversity control. Opossum was used for MOEA/D and RBFMOpt because it provides a modular platform capable of supporting both decomposition-based optimization and surrogate-assisted search strategies within the Grasshopper environment. The choice of plug-ins was based on their compatibility with the selected algorithms and their ability to integrate seamlessly with the parametric model and constraint evaluation logic.

Following recommendations from previous studies [50], simulations were conducted targeting 1,500 generated solutions. For NSGA-III optimization using the Tunny plug-in generation size was set to 50 while crossover and mutation rates were maintained at the plugin's default values (Crossover probability: 0,9; Swapping probability:0,5; Crossover type: Uniform). For RBFMOpt optimization using the Opossum plugin, the maximum number of true evaluations was set to 150, also using default evolutionary operator settings (Max cycles:1; Weight method: Tchebycheff; Epsilon:0,1). For MOEA/D optimization, also conducted using Opossum, the user is limited to controlling only the total number of evaluations, which was likewise set to 1,500.

To enable an evaluation of how different GD algorithms interact with the parametric model, a structured set of data was extracted from each optimization run. The extracted data was selected to allow detailed analysis of both search behavior and optimization outcomes. Specifically, objective values (O1–O5) for each generated solution were recorded to reconstruct Pareto fronts and analyze trade-offs between competing criteria; parameter values for each generated solution were captured to assess how the algorithms modified design parameters over time; and generation number and computational time were also recorded to reconstruct the temporal evolution of the search. From this dataset, several types of analytical visualizations were constructed, including objective space scatter plots illustrating the distribution and trade-offs between selected objective pairs, parameter evolution diagrams tracking how key parameters were modified across generations, and objective value evolution diagrams showing how performance metrics evolved during the optimization process. This combination of quantitative and visual analyses provides a foundation for evaluating how each algorithm navigated the parametric design space. The assessment focused on how parameter values evolved over time, how objectives interacted during optimization, and how solution diversity and convergence behavior developed under a fixed evaluation budget. In addition to evaluating algorithmic performance, the extracted data also serves to provide insights into the relationship between the parametric model structure and generative search behavior.

4 RESULTS

Each of the three optimization algorithms (NSGA-III, MOEA/D, and RBFMOpt) were applied to the parametric model of the dental abutment in two distinct clinical cases. In both cases, simulations were configured to generate 1,500 solutions per algorithm. All algorithms successfully produced solution sets without regeneration errors or computational interruptions. Table 2 summarizes the best objective values achieved for each algorithm in both test cases, along with the corresponding computation times. Figures 8 and 9 illustrate representative abutment geometries produced by each algorithm for Case 1 and Case 2, respectively.

NSGA-III generally achieved balanced performance across all objectives in both cases, particularly maintaining competitive results on O1–O4 and consistently low values for O5, especially in Case 2. RBFMOpt demonstrated excellent performance on the PCS-related objective O5 in both cases, achieving the lowest apex position error overall, but required longer computation times compared to both NSGA-III and MOEA/D. MOEA/D performed well on selected objectives, particularly O3 and O4 in Case 2, but showed greater variability and higher O5 values.

Algorithm	Case	O1 best value [mm]	O2 best value [mm]	O3 best value [mm]	O4 best value [mm]	O5 best value [mm]	Computation time
NSGA-III	1	0,3691	0,0288	0,0358	0,0282	0,1505	26:28
MOEA/D		0,3729	0,0537	0,0374	0,0497	0,1403	10:08
RBFMOpt		0,3685	0,0268	0,0004	0,0268	0,0018	31:05
NSGA-III	2	0,348972	0,041539	0,060481	0,254153	0,105210	35:42
MOEA/D		0,342692	0,083449	0,079779	0,254872	0,042674	12:04
RBFMOpt		0,329191	0,039348	0,012764	0,251246	0,003407	28:51

Table 2. Overview of algorithm performance.

The convergence behavior of objective values (O1 to O5) for the three tested algorithms—NSGA-III, MOEA/D, and RBFMOpt is presented in Figures 10 to 15. These diagrams illustrate how each algorithm performed across both test cases when optimizing the parametric model. A general pattern observed across all algorithms is the rapid and consistent convergence of objectives O1 to O4, which relate to the emergence profile and are primarily influenced by independently adjustable transgingival parameters. In contrast, objective O5, associated with the

apex positioning of the prosthetic connection segment (PCS), consistently exhibited slower and more irregular convergence, reflecting its greater sensitivity to global geometric interactions and parameter coupling.

Figure 8. Generated abutments by each algorithm in Case 1 (NSGA-III – left; MOAE/D – middle; RBFMOpt – right).

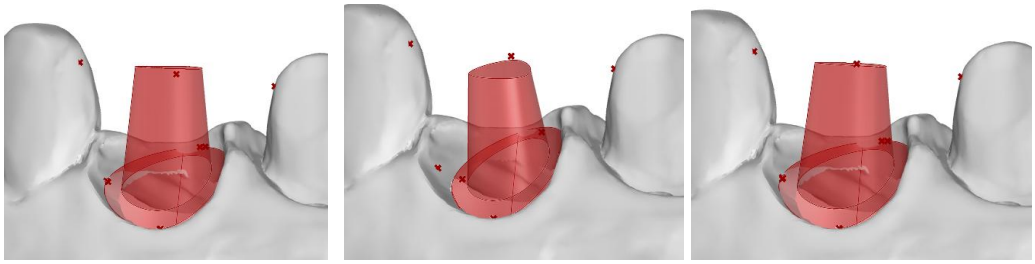

Figure 9. Generated abutments by each algorithm in Case 2 (NSGA-III – left; MOAE/D – middle; RBFMOpt – right).

Comparative analysis highlights distinct differences in algorithm behavior. NSGA-III demonstrated the most balanced performance across all objectives, including consistent refinement of O5. MOEA/D showed strong early-stage improvements but required more evaluations to stabilize O5. RBFMOpt achieved fast early convergence across all objectives, including O5, though with less refinement in the later stages. These observations underscore the influence of algorithmic search strategy on handling differently structured objectives and set the context for the case-specific analyses that follow.

The convergence behavior of objective values for NSGA-III across both tested cases is presented in the figures 11 and 11. In Case 1 (Figure 10), all five objectives show a steep initial drop in the first 100 solutions, followed by a more gradual decline. The convergence for the emergence profile objectives (O1 to O4) begins stabilizing after 525 solutions. By this point, O2, O3 and O4 reach values below 0,05 mm, and O1 approaches 0,4 mm. O5, representing the PCS apex positioning, remains elevated beyond 0,5 mm until around solution 300, after which it gradually approaches its minimum of 0,151 mm. The convergence of O5 is more delayed and irregular, indicating its higher sensitivity to parameter interactions and the complexity of global geometric dependencies.

In Case 2 (Figure 11), the objective values show a steep decline within the first 100 solutions, similar to the pattern observed in Case 1. O1 converges very early, stabilizing after only about 20 solutions, indicating that the initial point in the parametric model was already positioned close to an optimal region of the design space. O2 and O3 stabilize by approximately solution 310, reaching minimal values below 0,05 mm. O4 converges around solution 260, with a final value of 0.265 mm. The O5 objective again displays delayed convergence. Its minimum value of 0,105 mm is not reached until after solution 1218, at which point it stabilizes. Between solutions 650 and 1200, O5 exhibits three distinct drops in value, further confirming the complexity and sensitivity of this objective, as was also evident in Case 1.

Figures 12 and 13 illustrate the convergence behavior of objective values O1 to O5 across the sequence of 1,500 generated solutions for Case 1 and Case 2 using MOEA/D algorithm.

In Case 1 (Figure 12), O1 and O5 show a steep reduction in value during the initial 50 solutions which exhibit the highest initial values and the most pronounced early drops. By solution 270, objectives O1 to O4 approach convergence, with minimal improvements observed beyond solution 680. This indicates that the algorithm has effectively converged to a stable region of the solution space relatively early in the evaluation process. The convergence of O5 is again delayed compared to the other objectives, with adjustments continuing up to around 900 solutions before fully stabilizing. Final objective values for Case 1 are: O1 = 0,3729 mm, O2 = 0,0537 mm, O3 = 0,0374 mm, O4 = 0,0497 mm, and O5 = 0,1403 mm.

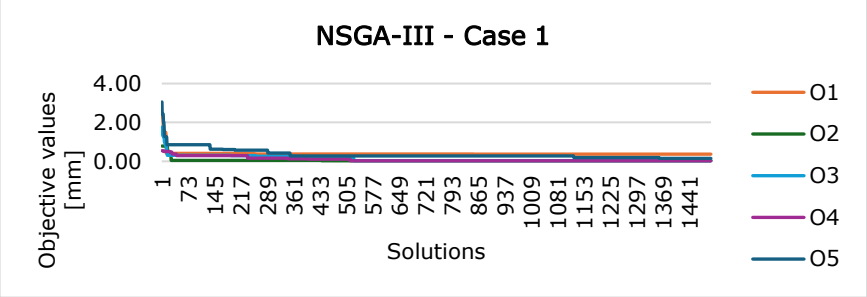

Figure 10. Convergence of objective values – NSGA-III – Case 1.

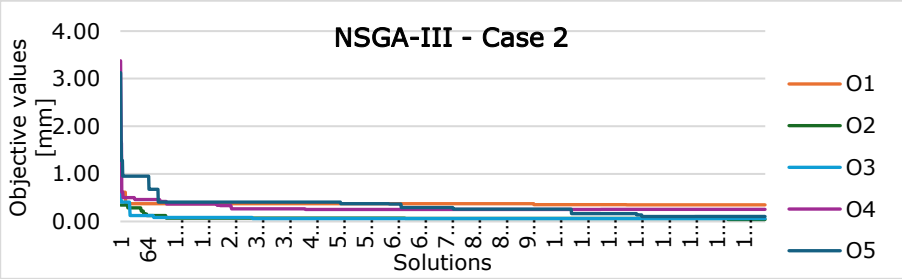

Figure 11. Convergence of objective values – NSGA-III – Case 2.

In Case 2 (Figure 13), a similar convergence pattern is observed. Objective values undergo substantial reduction in the first 150 solutions, particularly O1 and O5. Around solution 630, most objectives stabilize, with O5 again showing a slightly delayed convergence compared to the others. Final objective values for Case 2 appear to converge somewhat earlier than in Case 1, suggesting a potentially smoother optimization landscape for this scenario. Final objective values for Case 2 using MOEA/D algorithm were: O1 = 0,3427 mm, O2 = 0,0834 mm, O3 = 0,0779 mm, O4 = 0,2549 mm, and O5 = 0,0427 mm.

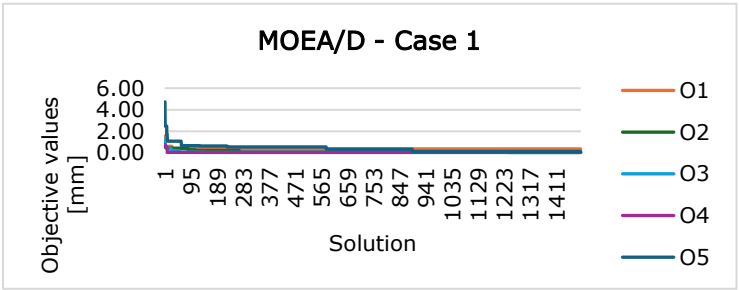

Figure 12. Convergence of objective values – MOAE/D – Case 1.

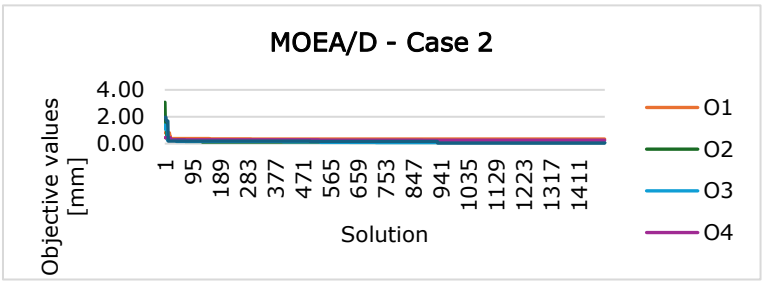

Figure 13. Convergence of objective values – MOAE/D – Case 2.

Figures 14 and 15 present the convergence behavior of objective values O1 to O5 for the RBFMOpt algorithm in Case 1 and Case 2. In Case 1 (Figure 14), all objectives show a rapid initial decrease, with convergence occurring before approximately solution 100. O1 stabilizes early, reaching 0,3685 mm by solution 120. O2 and O3 initially

stabilize after solution 150, reaching values of 0,046 mm and 0,022 mm, respectively. From that point until the end of the optimization, both continue to converge gradually toward final values of O2 = 0,027 mm and O3 = 0,0004 mm. O4 reaches 0,0268 mm at solution 394 and remains unchanged thereafter. O5 shows a small secondary refinement phase around solution 330, where it reaches 0,075 mm, and ultimately converges to 0,0018 mm by the end of the run.

In Case 2 (Figure 15), convergence is even faster and more uniform than in Case 1. All five objectives reach initial stabilization by approximately solution 80, with only O5 exhibiting a more pronounced secondary refinement phase after solution 640. Final objective values are: O1 = 0,3292 mm, O2 = 0,0393 mm, O3 = 0,0128 mm, O4 = 0,2512 mm, and O5 = 0,0034 mm.

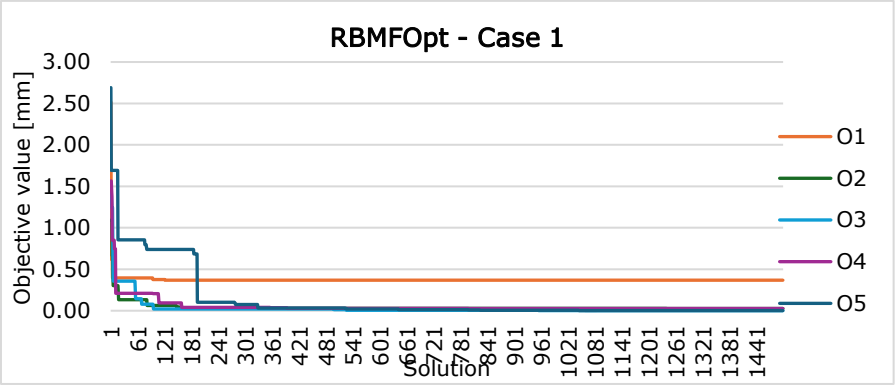

Figure 14. Convergence of objective values – RBFMOpt – Case 1.

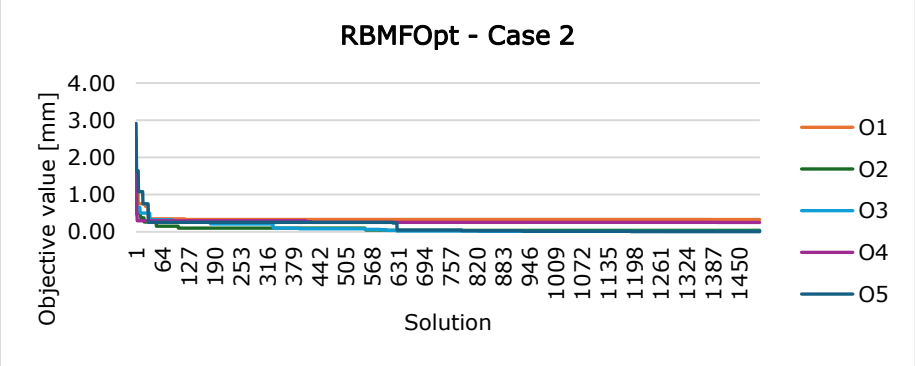

Figure 15. Convergence of objective values – RBFMOpt – Case 2.

Figures 16, 17 and 18 present the objective space correlation plots for the O1 and O5 objective pair across all three optimization algorithms, NSGA-III, MOEA/D, and RBFMOpt, evaluated under both test cases. This objective pair was selected for closer analysis because it represents a structurally more complex interaction between localized emergence profile shaping and global spatial alignment. O1 (distal emergence profile deviation) and O5 (PCS apex positioning) are connected through the geometry at the transition between the TGS and PCS, where changes in the emergence margin will influence the orientation and endpoint of the PCS axis. While all four TGS-related objectives (O1–O4) likely contribute similarly to this interaction, O1 was selected as a representative objective to illustrate how algorithms manage trade-offs between local soft-tissue conformity and global prosthetic alignment. In contrast, objective pairs such as O1–O2 or O2–O3 involve only locally optimized surfaces and offer less insight into how algorithms handle interdependent objectives across geometric regions. By focusing on O1–O5, we highlight a scenario where competing spatial demands must be resolved within a constrained parametric model, serving as a more illustrative case for analyzing generative search behavior.

Figure 16 shows the distribution of solutions in the O1–O5 objective space for NSGA-III. In both cases, the solution sets are concentrated toward the lower-left quadrant of the plot, suggesting that NSGA-III was able to simultaneously reduce both objectives to low values in a significant portion of the population. This clustering indicates that the algorithm effectively explored regions of the design space where emergence profile fitting and apex positioning were jointly optimized, despite the structural complexity introduced by their interdependence. The distribution is denser and more compact in Case 1, with a larger number of solutions falling below 1,5 mm in both O1 and O5. In Case 2, although the overall pattern is similar, the spread of solutions is slightly wider,

particularly along the O5 axis, reflecting increased difficulty in aligning the PCS apex due to anatomical constraints in the anterior region. Still, the algorithm maintains a relatively smooth front of high-quality trade-offs, showing that NSGA-III preserved diversity while converging toward effective compromises. Importantly, the lack of a sharp trade-off curve or narrow frontier confirms that O1 and O5 are not in strict conflict but rather represent a loosely coupled optimization scenario.

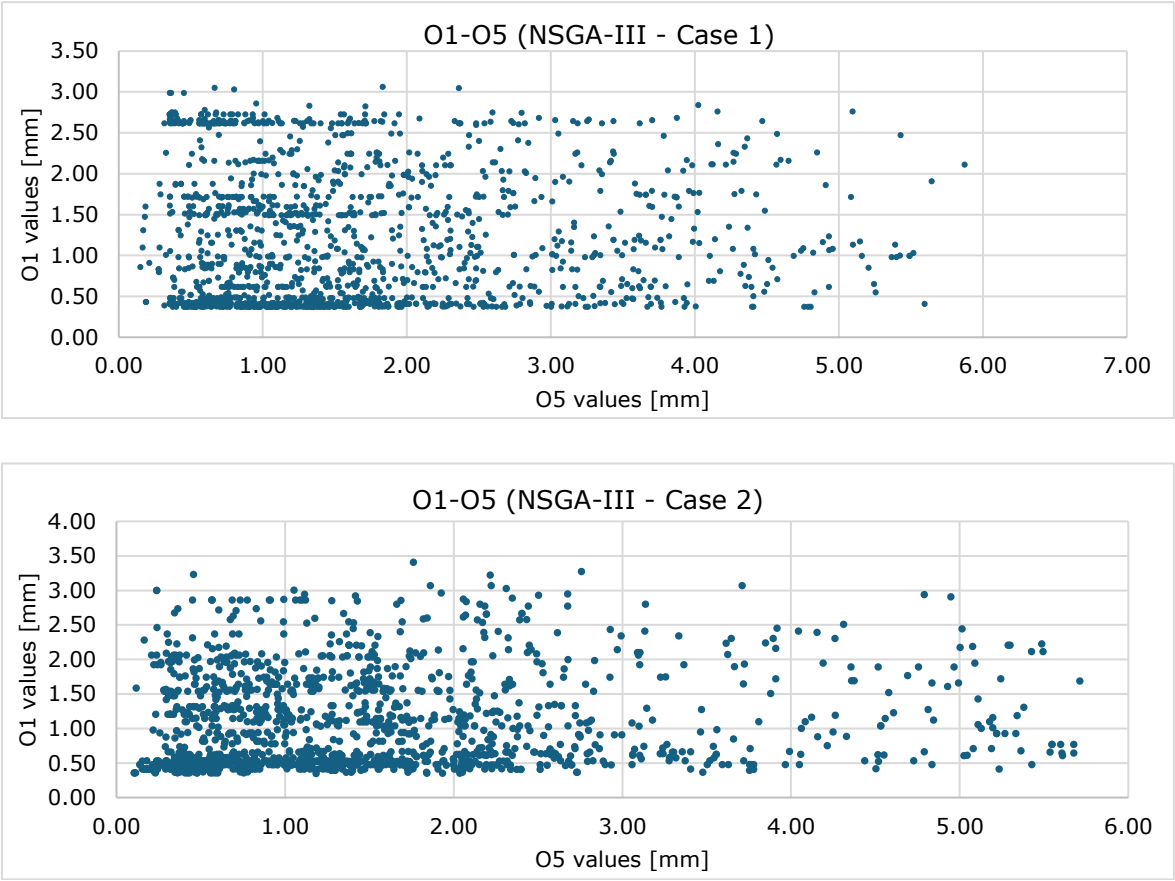

Figure 16. Objective correlation plots - NSGA-III.

Compared to NSGA-III, the solution sets generated by MOEA/D (Figure 17) are more widely scattered across the objective space, with less clear clustering toward the lower-left region where both objectives are minimized. A significant portion of solutions display low O1 values (below 1,5 mm) but relatively high O5 values, suggesting that MOEA/D struggled to coordinate improvements between the local and global objectives effectively.

The pattern is even more pronounced in Case 2, where the distribution of solutions becomes broader across both axes. Here, higher O5 variability is accompanied by increased scatter in O1 values as well, with fewer solutions achieving simultaneous minimization of both objectives. This result points to challenges in navigating the more complex spatial constraints imposed by the anterior region anatomy, where small changes in local emergence profile parameters have a more pronounced effect on the global alignment of the PCS axis. The decomposition-based nature of MOEA/D, which optimizes scalar subproblems associated with specific weight vectors, may have contributed to this behavior. While effective in guiding solutions toward individual trade-off directions, MOEA/D appears less capable of maintaining coordinated improvements across loosely coupled, multi-scale objectives like O1 and O5. As a result, the search process may have fragmented into subregions, preventing effective convergence toward broad exploration of the solution space.

Figure 18 presents the distribution of solutions in the O1–O5 objective space for RBFMOpt across both test cases. The solution generated through surrogate-assisted optimization exhibits a different distribution of solutions compared to evolutionary algorithms. In Case 1, a distinct concentration of solutions achieving lower O5 values is visible, with many solutions falling below 2.0 mm in apex positioning deviation. However, these improvements in O5 are not always accompanied by correspondingly low O1 values. The spread along the O1 axis is broader than in NSGA-III, indicating that while the surrogate model effectively guided the search toward better apex alignment, emergence profile conformity was less consistently optimized.

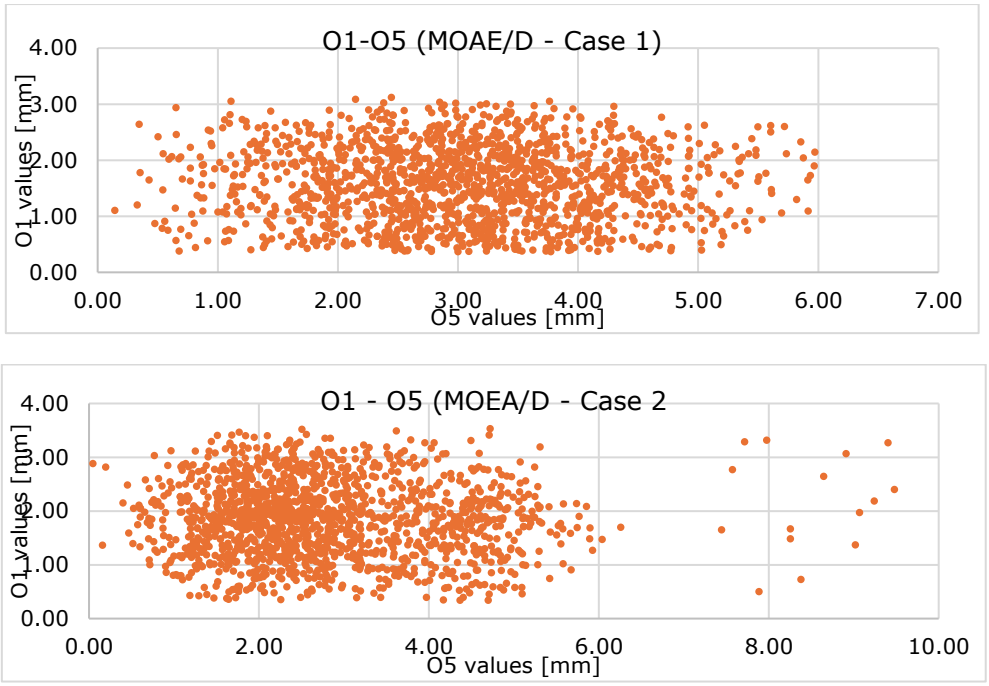

Figure 17. Objective correlation plots - MOEA/D

A similar pattern is observed in Case 2, where apex positioning shows relatively better clustering compared to MOEA/D but again with greater variability in emergence profile fitting. The surrogate appears to prioritize improvements in O5 earlier in the search process, consistent with the strength of surrogate-assisted strategies in quickly exploiting promising regions. However, achieving balanced solutions across both local (O1) and global (O5) objectives appears more challenging as the search progresses. This behavior can be attributed to the nature of surrogate-based optimization. While the surrogate model enables efficient exploration by reducing the number of evaluations, its approximation accuracy can diminish in complex, non-linear regions of the objective space, particularly when objectives are interdependent across different spatial scales. As the search targets for longer trade-offs between local surface fitting and apex positioning, surrogate inaccuracies may prevent consistent refinement of both objectives simultaneously.

5 DISCUSSION

The results presented in this study reveal distinct behaviors across NSGA-III, MOEA/D, and RBFMOpt when applied to a parametric model of a custom dental abutment. While the quantitative differences in objective errors and solution distributions are evident, a deeper analysis shows that these outcomes are strongly rooted in the intrinsic search strategies of each algorithm, the complexity of the design objectives, and the parametric structure of the model itself.

The convergence behavior of objectives O1–O4 across all algorithms reflects the underlying simplicity of localized emergence profile adaptation tasks. These objectives are based on independently adjustable parameters, resulting in a relatively smooth and well-behaved optimization landscape. This aligns with findings from previous studies [23,37] that highlight the importance of low-dimensional, low-interdependence parameterizations for efficient generative search. In contrast, the O5 objective, relating to PCS apex positioning, consistently proved more challenging, due to its dependence on the adjustment of multiple global parameters (A_X, A_Y, CH). Such global geometric objectives create rugged solution spaces where surrogate inaccuracies, decomposition limitations, or inadequate diversity management can critically impair search performance [33,37].

NSGA-III's superior performance in terms of convergence, diversity, and robustness across objectives can be attributed to its reference-point-based non-dominated sorting strategy. Rather than producing a uniform spread, the algorithm progressively develops solutions across generations, with each iteration contributing to a more comprehensive and structured exploration of the objective space. This allowed NSGA-III to effectively manage the partial decoupling between local (O1–O4) and global (O5) objectives, maintaining a balance between exploration and convergence without becoming trapped in suboptimal regions. These findings are consistent with previous studies [27] that emphasize NSGA-III's strengths in complex, many-objective problems where maintaining diversity is critical. In contrast, MOEA/D's weaker performance, especially regarding O5, can be explained by its scalar decomposition approach. Although decomposition is effective for problems with well-

defined trade-off directions, it struggles when objectives interact non-linearly or when different objectives operate at different geometric scales. The high dispersion seen in MOEA/D's solution sets, particularly in the anterior case, illustrates its limitations when faced with design spaces where simple linear aggregation cannot capture the true multi-objective topology [34]. RBFMOpt demonstrated early and aggressive convergence toward low O5 values, outperforming the evolutionary algorithms in apex positioning precision. However, surrogate-assisted optimization also introduced limitations. While surrogate models can efficiently approximate smooth objective spaces [35], their accuracy diminishes in rugged, sensitive regions, leading to stagnation or unbalanced exploration [5]. Surrogate guidance prioritized apex positioning at the expense of greater variability in emergence profile fitting (O1–O4), particularly in Case 2. This behavior aligns with findings in surrogate-assisted optimization literature [5], where surrogate models may introduce biases favoring objectives with more predictable gradients.

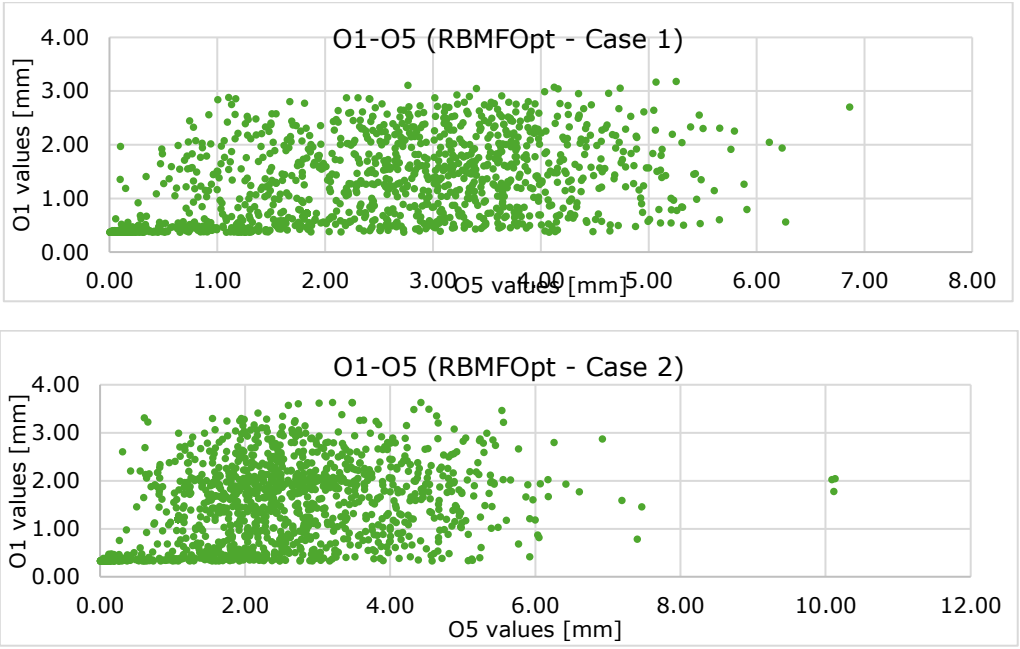

Figure 18. Objective correlation plots – RBMFOpt.

These differences underscore the importance of matching algorithmic strategies to the specific characteristics of the parametric model structure. Algorithms that combine strong diversity maintenance with effective multi-objective convergence, such as NSGA-III, appear better suited for parametric models involving both localized and global spatial optimization challenges.

Beyond algorithmic behavior, the results indicate that the preparation and structure of the parametric model fundamentally influence the effectiveness of GD workflows. The observed disparity between the convergence rates of emergence profile objectives (O1–O4) and PCS apex positioning (O5) directly reflects how parameters influence geometry, whether through localized or global control. In the transgingival segment (TGS), parameters were designed to adjust specific local features (lateral and vertical offsets at discrete anatomical directions), enabling proportional geometric adaptations. This produced a continuous solution space where generative algorithms could operate efficiently. In contrast, the prosthetic connection segment (PCS) was defined using angulation and height parameters (A_X, A_Y, CH), where small parametric changes caused large, often unpredictable shifts in apex positioning. This global dependency introduced ruggedness into the solution space, making optimization more complex and sensitive to search strategy deficiencies.

These findings reinforce that parametric models intended for GD must carefully balance variability and predictability [37]. Regions requiring fine-tuned spatial control should be structured with tighter parametric coupling, more predictable and continuous geometric behavior in response to parameter changes, and stricter bounding of allowable variations to support robust generative exploration. The study yields several concrete indications for designers working with constraint-aware parametric models:

- Where feasible, parameters should control local geometric features without cascading effects on distant regions. Localized control enables smoother optimization and reduces the risk of destabilizing the model, causing unintended geometric distortions, constraint violations, or numerical instability during generative exploration. In the case of the TGS, localized offsets and heights enabled fast, stable convergence of emergence margin curve fitting objectives.

- When global geometric dependencies are unavoidable, such as in PCS apex positioning, designers must recognize that these areas will inherently create more complex optimization challenges. Parameters controlling such features should be carefully bounded to avoid excessive variability, and additional geometric constraints or penalties may be needed to stabilize the search.
- Building parametric models hierarchically, where foundational geometric features are established first and dependent features are constructed upon stable references, can greatly enhance model robustness during optimization. In this study, defining the TGS emergence margin curve before constructing the PCS vector ensured that core anatomical adaptation was preserved even when PCS variation became aggressive.
- Designers should not assume that all design objectives will be equally tractable during generative search. Objectives involving local surface fitting (e.g., emergence margin curve) tend to be easier to optimize because they are influenced by a small number of localized parameters and have smooth, predictable behavior. In contrast, objectives involving global spatial alignment (e.g., PCS apex positioning) are affected by multiple interdependent parameters, often exhibit nonlinear behavior, and are more prone to violating geometric or functional constraints. These characteristics increase the complexity of the search process and typically require more advanced algorithmic support and extended evaluation time. Recognizing these differences in advance enables more realistic expectations regarding optimization difficulty and resource allocation.
- While much attention should be placed on algorithm selection, the effectiveness of generative workflows is ultimately limited or enabled by the quality of the parametric model itself. A clear, constraint-aware, sensitivity-managed model (a model in which parameter changes produce predictable, proportional, and stable geometric responses) dramatically reduces optimization complexity, improves convergence reliability, and enhances the interpretability of generated solutions. A poorly structured model can confuse even the most advanced algorithms

This study highlights that in generative engineering design, the parametric model plays a critical role in shaping the behavior and performance of optimization algorithms. The model's structure defines the topology of the design space, its parameter sensitivity influences the complexity of the optimization landscape, and embedded constraints determine the bounds of feasible exploration. As such, preparing the parametric model should not be viewed solely as a geometric task, but as a strategic design activity that affects the efficiency and outcome of the generative process. While algorithm selection remains important, careful attention to model preparation can substantially improve convergence behavior and the quality of generated solutions.

6 CONCLUSIONS

This study explored the application of three GD algorithms, NSGA-III, MOEA/D, and RBFMOpt, to a parametric model of a custom dental abutment. Through controlled optimization experiments focusing on geometrical performance objectives, the research investigated not only algorithmic behavior but also the deeper relationship between parametric model structure and generative search dynamics. The results showed that local geometric objectives, such as emergence margin curve fitting (O1–O4), were generally easier to optimize, exhibiting fast and stable convergence across all tested algorithms. In contrast, global spatial objectives, such as PCS apex positioning (O5), proved significantly more challenging due to the non-linear and sensitive relationship between design parameters and apex location. Among the tested algorithms, NSGA-III demonstrated the most consistent and effective search behavior, achieving faster convergence and better Pareto front structuring compared to MOEA/D and RBFMOpt. Beyond algorithmic comparison, the study highlighted the crucial role of parametric model preparation in enabling successful generative workflows. Models structured with localized control, smooth parameter-to-geometry mapping, and hierarchical dependency management facilitated more efficient and reliable optimization. In contrast, models embedding global dependencies without sufficient constraint management introduced greater complexity and sensitivity, challenging even advanced optimization strategies. These findings suggest that in engineering applications where constrained mechanical components must be optimized within anatomically or functionally complex environments, the design of the parametric model is as important as the selection of the optimization algorithm. Careful segmentation, thoughtful parameter bounding, and sensitivity anticipation are key strategies for creating generative-ready models that support stable and meaningful exploration.

Future work will extend this research by integrating additional objective functions into the GD process, expanding beyond geometric objectives to include structural performance, manufacturing feasibility, prosthetic assembly requirements, and aesthetic considerations. Building on this expanded objective space, subsequent work will explore hybrid optimization strategies that combine multiple algorithms within a single workflow to improve convergence behavior, solution diversity, and robustness. Data-driven GD approaches, incorporating machine learning models or prior case data, will also be investigated to complement parametric workflows and reduce evaluation costs. Additionally, to further improve the model based on the observations gathered during this study, alternative parametric model configurations will be prepared and analyzed to derive actionable

recommendations for model structure, parameterization strategies, and constraint embedding, with the aim of improving generative performance across diverse engineering contexts. This research also presented advantages and disadvantages between different generative algorithms where RBMFOpt showed greater convergence rates while giving accurate final outputs early in the process, however it showed limitations when dealing with complex objectives. On the other hand, NSGA-III shows better solution space exploration even in complex objectives but requires larger number of solutions to converge. This emphasizes that in order to be able to give practitioners recommendations on how to choose generative algorithms in this context, future research should analyze both algorithms when the model complexity increases. Collectively, these directions aim to broaden the applicability and industrial readiness of GD, both within dentistry and in other domains where constrained personalization is required.

7 ACKNOWLEDGEMENTS

This paper was funded by the European Union and National Recovery and Resilience Plan project, reference number: NPOO.C3.2.R3-I1.04.0121 - Generative Design for Mass Personalization of Dental Implantoprosthetic Abutments (GENKON).

REFERENCES

[1] Bandi, A.; Adapa, P. V. S. R.; Kuchi, Y. E. V. P. K.: The Power of Generative AI: A Review of Requirements, Models, Input–Output Formats, Evaluation Metrics, and Challenges, Futur Internet, 15 (8), 2023, 260.
[2] Banerjee, A.; Pradhan, S.; Misra, B.; Chakraborty, S.: Applied Multi-objective Optimization, Springer Tracts Nat-Inspir Comput, 2024, 1–19.
[3] Belluomo, L.; Trovato, M.; Bici, M.; Cicconi, P.; Campana, F.: An Iterative Generative Design Approach for Multi-Material Components, Comput-Aided Des Appl, 2024, 1089–102.
[4] Binder, J.; Unver, E.; Olaosun, D.; Geren, N.: Qualitative Data-Driven Generative Design for Personalized Wearable Scalp Cooling Devices, Comput-Aided Des Appl, 2024, 261–71.
[5] Bliek, L.; Guijt, A.; Karlsson, R.; Verwer, S.; Weerdt, M. de: Benchmarking surrogate-based optimization algorithms on expensive black-box functions, Appl Soft Comput, 147, 2023, 110744.
[6] Caetano, I.; Santos, L.; Leitão, A.: Computational design in architecture: Defining parametric, generative, and algorithmic design, Front Arch Res, 9 (2), 2020, 287–300.
[7] Camba, J. D.; Contero, M.; Company, P.: Parametric CAD modeling: An analysis of strategies for design reusability, Comput-Aided Des, 74, 2016, 18–31.
[8] Chang, H.; Sun, Y.; Lu, S.; Lin, D.: Application of non-dominated sorting genetic algorithm (NSGA-III) and radial basis function (RBF) interpolation for mitigating node displacement in smart contact lenses, Sci Rep, 14 (1), 2024, 29348.
[9] Chang, K. H.: Design Theory and Methods Using CAD/CAE, 2015, 103–210.,
[10] Chansoria, S.; Chansoria, H.: Abutment Selection In Fixed Partial Denture, IOSR-JDMS, 2018. https://doi.org/10.9790/0853-1703010412
[11] Chen, Y.; Yin, X.; Xiao, B.; Shen, Y.; Liu, H.; Gradišar, L.; et al.: Generative Design Methodology and Framework Exploiting Designer-Algorithm Synergies, Buildings 2022, Vol 12, Page 2194, 12, 2022, 2194. https://www.mdpi.com/2075-5309/12/12/2194/htm
[12] Cho, J. H.; Wang, Y.; Chen, I. R.; Chan, K. S.; Swami, A.: A Survey on Modeling and Optimizing Multi-Objective Systems, IEEE Commun Surv Tutor, 19 (3), 2017, 1867–901.
[13] Cirello, A.; Ingrassia, T.; Marannano, G.; Mirulla, A. I.; Nigrelli, V.; Petrucci, G.; et al.: A New Automatic Process Based on Generative Design for CAD Modeling and Manufacturing of Customized Orthosis, Appl Sci, 14 (14), 2024, 6231.
[14] Costa, A.; Nannicini, G.: RBFOpt: an open-source library for black-box optimization with costly function evaluations, Math Program Comput, 10 (4), 2018, 597–629.
[15] Deb, K.; Deb, K.: Search Methodologies, Introductory Tutorials in Optimization and Decision Support Techniques, 2013, 403–49.
[16] Deb, K.; Jain, H.: An Evolutionary Many-Objective Optimization Algorithm Using Reference-Point-Based Nondominated Sorting Approach, Part I: Solving Problems With Box Constraints, IEEE Trans Evol Comput, 18 (4), 2014, 577–601.
[17] Deb, K.; Pratap, A.; Agarwal, S.; Meyarivan, T.: A Fast and Elitist Multiobjective Genetic Algorithm: NSGA-II, IEEE Trans Evol Comput, 6 (2), 2002, 182.
[18] Dong, Z.; Wang, X.; Tang, L.: MOEA/D with a self-adaptive weight vector adjustment strategy based on chain segmentation, Inf Sci, 521, 2020, 209–30.
[19] Farzane, K.; B, D. A.: A review and evaluation of multi and many-objective optimization: Methods and algorithms, Glob J Ecol, 7 (2), 2022, 104–19.

[20] Grigorenko, A.; Shopina, E.: Generative design and adaptation for manufacturing of steering knuckle. Part ii, Bull Belgorod State Technol Univ named after V G Shukhov, 8 (2), 2022, 102–12.
[21] Gu, N.; Yu, R.; Behbahani, P. A.: Parametric Design: Theoretical Development and Algorithmic Foundation for Design Generation in Architecture, 2018, 1–22.
[22] Han, Z. H.; Zhang, K. S.: Real-World Applications of Genetic Algorithms, 2012.
[23] Harding, J. E.; Shepherd, P.: Meta-Parametric Design, Des Stud, 52, 2017, 73–95.
[24] Ibrahim, N.; Cox, S.; Mills, R.; Aftelak, A.; Shah, H.: Multi-objective decision-making methods for optimising CO2 decisions in the automotive industry, J Clean Prod, 314, 2021, 128037.
[25] Jaisawal, R.; Agrawal, V.: Generative Design Method (GDM) – A State of Art, IOP Conf Ser: Mater Sci Eng, 1104 (1), 2021, 012036.
[26] Jones, D. F.; Florentino, H. O.: The Palgrave Handbook of Operations Research, 2022, 181–207.
[27] Khamaru, K.; Wainwright, M. J.: Convergence guarantees for a class of non-convex and non-smooth optimization problems, arXiv, 2018,
[28] Kim, J.; Kwon, Y.; Kang, N.: Deep Generative Design for Mass Production, arXiv, 2024,
[29] Kok, I. J. D.; Katz, L. H.; Duqum, I. S.: CAD/CAM Custom Abutments for Esthetic Anterior Implant-Supported Restoration: Materials and Design, Curr Oral Heal Rep, 5 (2), 2018, 121–6.
[30] Kosec, P.; Huić, I.; Gulin, F.; Škec, S.: Kosec - Towards systematic approach of mass customization in dental prosthetics.pdf, In: Anisic Z, Forza C, editors. Proceedings of the MCP 2024 Conference, Novi Sad. Serbia; 2024. https://mcp-ce.org/wp-content/uploads/2024/11/23_Kosec.pdf
[31] Krish, S.: A practical generative design method, Comput-Aided Des, 43 (1), 2011, 88–100.
[32] Li, H.; Lachmayer, R.: Automated Exploration of Design Solution Space Applying the Generative Design Approach, Proc Des Soc: Int Conf Eng Des, 1 (1), 2019, 1085–94.
[33] Li, H.; Ye, Y.; Zhang, Z.; Yu, W.; Zhu, W.: A comparative analysis of CAD modeling approaches for design solution space exploration, Adv Mech Eng, 16 (3), 2024, 16878132241238088.
[34] Li, K.: A Survey of Decomposition-Based Evolutionary Multi-Objective Optimization: Part I-Past and Future, arXiv, 2024.
[35] Liu, S.; Wang, H.; Peng, W.; Yao, W.: Surrogate-assisted evolutionary algorithms for expensive combinatorial optimization: a survey, Complex Intell Syst, 10 (4), 2024, 5933–49.
[36] McKnight, M.: Generative Design: What it is? How is it being used? Why it's a game changer, KnE Eng, 2 (2), 2016, 176–81.
[37] Mountstephens, J.; Teo, J.: Progress and Challenges in Generative Product Design: A Review of Systems, Computers, 9 (4), 2020, 80.
[38] Nordin, A.: Challenges in the industrial implementation of generative design systems: An exploratory study, Artif Intell Eng Des, Anal Manuf, 32 (1), 2018, 16–31.
[39] Papallo, I.; Martorelli, M.; Lamonaca, F.; Gloria, A.: Generative design and insights in strategies for the development of innovative products with tailored mechanical and/or functional properties, Acta IMEKO, 12 (4), 2023, 1–5.
[40] Pereira, J. L. J.; Oliver, G. A.; Francisco, M. B.; Cunha, S. S.; Gomes, G. F.: A Review of Multi-objective Optimization: Methods and Algorithms in Mechanical Engineering Problems, Arch Comput Methods Eng, 29 (4), 2022, 2285–308.
[41] Pomazan, V. M.; Sintea, S. R.: Generative design for assembly wrapping up, IOP Conf Ser: Mater Sci Eng, 916 (1), 2020, 012086.
[42] Ramesh, B.; RJ, A.; Singla, A.; Chandra, P. K.; Sethi, V. A.; Abood, A. S.: Utilizing Generative Design Algorithms for Innovative Structural Engineering Solutions, E3S Web Conf, 505, 2024, 03010.
[43] Rawat, A. S.; Tiwari, G.: Advances in Engineering Design, Select Proceedings of FLAME 2022, Lect Notes Mech Eng, 2023, 275–84.
[44] Regenwetter, L.; Nobari, A. H.; Ahmed, F.: Deep Generative Models in Engineering Design: A Review, J Mech Des, 144 (7), 2022.
[45] Saadi, J. I.; Yang, M. C.: Generative Design: Reframing the Role of the Designer in Early-Stage Design Process, J Mech Des, 145 (4), 2023.
[46] Silva, M. A. da; Garcia, R. de P.; Carlo, J. C.: Performance assessment of RBFMOpt, NSGA2, and MHACO on the thermal and energy optimization of an office building, J Build Perform Simul, 16 (3), 2023, 366–80. https://doi.org/10.1080/19401493.2022.2143568
[47] Starodubcev, N. O.; Nikitin, N. O.; Andronova, E. A.; Gavaza, K. G.; Sidorenko, D. O.; Kalyuzhnaya, A. V.: Generative design of physical objects using modular framework, Eng Appl Artif Intell, 119, 2023, 105715.
[48] Sun, L.; Zhang, B.; Wang, P.; Gan, Z.; Han, P.; Wang, Y.: Multi-Objective Parametric Optimization Design for Mirrors Combined with Non-Dominated Sorting Genetic Algorithm, Appl Sci, 13 (5), 2023, 3346. https://doi.org/10.3390/app13053346
[49] Wang, Z.; Pei, Y.; Li, J.: A Survey on Search Strategy of Evolutionary Multi-Objective Optimization Algorithms, Appl Sci, 13 (7), 2023, 4643. https://doi.org/10.3390/app13074643

[50] Wortmann, T.: Genetic evolution vs. function approximation: Benchmarking algorithms for architectural design optimization, J Comput Des Eng, 6 (3), 2019, 414–28. https://doi.org/10.1016/j.jcde.2018.09.001
[51] Xia, T.; Wang, L.; Xu, J.; Yuan, J.; Fu, Y.; Luo, Z.; et al.: A novel generative approach to the parametric design and multi-objective optimization of horizontal axis tidal turbines, Phys Fluids, 36 (11), 2024, 117118.
[52] Zhang, Q.; Li, H.: MOEA/D: A Multiobjective Evolutionary Algorithm Based on Decomposition, IEEE Trans Evol Comput, 11 (6), 2007, 712–31., https://doi.org/10.1109/tevc.2007.892759
[53] Zhuang, X.; Ju, Y.; Yang, A.; Caldas, L.: Synthesis and generation for 3D architecture volume with generative modeling, Int J Arch Comput, 21 (2), 2023, 297–314.